International Journal of Computational and Theoretical Chemistry
2020; 8(1): 11-18
http://www.sciencepublishinggroup.com/j/ijctc
doi: 10.11648/j.ijctc.20200801.12
ISSN: 2376-7286 (Print); ISSN: 2376-7308 (Online)

Importance of Hydride-Hydride Interaction in the Stabilization of LiH, NaH, KH, $LiAlH_4$, $NaAlH_4$, and Li_3AlH_6 as Solid-State Systems for Hydrogen Storage

James Tembei Titah[1, *], Franklin Che Ngwa[1], Mamadou Guy-Richard Kone[2]

[1]Department of Chemistry, University of New Brunswick, Fredericton, Canada

[2]Faculty of Fundamental and Applied Sciences (UFR SFA), Nangui Abrogoua University, Abidjan, Ivory Coast

Email address:

tt.james@unb.ca (J. T. Titah), tijames2001@yahoo.com (J. T. Titah)

[*]Corresponding author

To cite this article:

James Tembei Titah, Franklin Che Ngwa, Mamadou Guy-Richard Kone. Importance of Hydride-Hydride Interaction in the Stabilization of LiH, NaH, KH, $LiAlH_4$, $NaAlH_4$, and Li_3AlH_6 as Solid-State Systems for Hydrogen Storage. *International Journal of Computational and Theoretical Chemistry.* Vol. 8, No. 1, 2020, pp. 11-18. doi: 10.11648/j.ijctc.20200801.12

Received: December 11, 2019; **Accepted**: December 24, 2019; **Published**: January 7, 2020

Abstract: The solid-state structures of LiH, NaH, KH, $LiAlH_4$, $NaAlH_4$ and Li_3AlH_6 have been explored in details as potential hydrogen-storage materials using computational electron density methods; the full-potential linearized augmented plane wave (FPLAPW) method plus local orbital (FPLAPW+lo) embodied in the WIEN2k package code. Topological analysis of their DFT-computed electron densities in tandem with Bader's Atoms in Molecules (AIM) theory reveals a plethora of stabilizing interactions some of which are really strong. With the exception of NaH and KH, which do not contain the hydride-hydride bonding, the rest of the metal hydrides; LiH, $LiAlH_4$, $NaAlH_4$ and Li_3AlH_6 show an increasing number of hydride-hydride interactions that contribute to the stabilization of their three-dimensional (3-D) solid-state structures. Even though these hydride-hydride interactions are weaker compared to the M-H counterparts, their multiplicity greatly contributes to the stability of these metal hydrides. Results from their electron density studies reveal that the number of hydride-hydride interactions in these binary and complex metal hydrides increase with the complexity of the solid-state structures. $LiAlH_4$ is more stable compared to $NaAlH_4$, Li_3AlH_6, and LiH. NaH and KH were seen to be the least stable solid-state structures. It is suggested that the presence of these hydride-hydride interactions play a significant role in the mediation or understanding of the reaction mechanism leading to the release of hydrogen from these solid-state systems.

Keywords: Atoms in Molecules, DFT Calculations, Electron Density, Hydride-hydride Interaction, Topological Analysis

1. Introduction

Much experimental research has been done and is ongoing to select potential solid-state systems (materials) for hydrogen storage, but the mechanism behind the release of hydrogen in these systems is still largely unclear. In addition, a major drawback for most of these systems is their inability to reversibly release hydrogen at ambient temperatures and pressures, thus usually requiring catalytic conditions to release any appreciable amounts of hydrogen. As a result, the temperatures and pressures required to release hydrogen from these systems are generally either too high or too low for on-board vehicular applications. In order to be suitable for vehicular applications, solid-state hydrogen storage materials are required to meet the requirements or targets proposed by the US Department of Energy (DOE), viz; a hydrogen storage capacity of at least 5.5 wt. %, low desorption temperature (between 60-120°C), low cost, and low toxicity (environmentally friendly) [1-5]. Metal hydrides are materials with potential use not only in automobiles but also in many other applications, such as in rechargeable batteries, fuel cells, refrigerators, heat storage, nuclear industry, sensors, optical switches and hydrogen purification [6, 7]. Binary and complex metal hydrides of period 2 and 3 metals are potential candidates for hydrogen storage and other mobile applications. LiH, NaH, AlH_3, MgH_2, $NaAlH_4$, $LiAlH_4$, $LiNH_2BH_3$, $LiNH_2$ and Li_2NH desorbs respectively 12.6, 4.2, 2.5, 10.1, 7.4, 10.6, 13.6, 8.7,

and 3.5 wt % of hydrogen at temperatures between 100 and 300°C. The chemical simplicity of these binary and complex solid-state systems as well as their high hydrogen contents and low desorption temperatures have prompted enormous research geared at improving and enhancing their thermodynamic, kinetic, and materials properties for use as hydrogen storage materials and other mobile applications [6, 7].

To expand on the immense continuous experimental research already conducted on these and similar metal hydrides to improve and modify their properties for hydrogen storage using periodic DFT calculations in conjunction with a topological analysis of the electron density derived from the Bader's Quantum Theory of Atoms in Molecules (QTAIM) approach [8, 9], we investigate the structures and properties of LiH, NaH, KH, $NaAlH_4$, $LiAlH_4$ and Li_3AlH_6. In this paper, topological analysis of the electron density of the solid-state structures of some binary and complex metal hydrides (LiH, NaH, KH, $LiAlH_4$, $NaAlH_4$, and Li_3AlH_6) will be discussed in an attempt to obtain a clearer picture of the stabilizing interactions or bonding and reaction pathways for the release of H_2 from these systems. These solid-state systems reveal a spectrum of previously unrecognized bonding interactions in addition to hydride-hydride interactions that involves the hydride moieties in the materials, some of which are as strong as their conventional Na–H, Li–H, Al-H and Mg–H counterparts [10-12].

The chemical and physical properties of molecules and solid-state systems is based on the nature of interactions that exist between the atoms. The theory of 'atoms in molecules' AIM [8] can be seen as an ongoing research that aims at extracting and interpreting chemical information from modern quantum mechanical techniques (ab initio wave function) in solids. It was propounded in the early 1970s by Richard Bader and co-worker [8], and is currently being used by more than 70 laboratories worldwide in areas of surface science, organometallic chemistry, life science, solid-state physics and chemistry, drug design, physical-organic chemistry, crystallography, etc. The theory provides a simple, rigorous and elegant way of analyzing and interpreting the various types of stabilizing interactions in solid-state materials (maintaining atoms individuality) from the electron density and its Laplacian [8, 13, 14].

2. Methodology

In this research, we used the full-potential linearized augmented plane wave (FPLAPW) method plus local orbital (FPLAPW+lo) embodied in the WIEN2k package code [15]. No shape approximations are applied for charge density or potential. The exchange-correlation effects are treated in the density functional theory (DFT) within the FPLAPW formalism, using the generalized gradient approximation (GGA) together with Perdew and Wang functional (PBE96) [16]. The crystal unit cell used in this approach is partitioned into non-overlap atomic spheres (muffin tins) and interstitial region. The radii of the muffin tin spheres are constrained by the requirement that they are non-overlapping and that the core states do not significantly spill into the interstitial region. Inside each muffin tin, orbitals are described as radial functions times spherical harmonics and a fully relativistic treatment is used, based on the work by Desclaux [17]. The interstitial region is described using plane waves and a scalar relativistic treatment is applied [18]. The wave functions of both regions are set to match in value and slope at the muffin tin boundaries, but a perfect match would require the inclusion of spherical harmonics to infinite order within each atomic sphere and a truncated series is instead used. Care must be taken to ensure that any remaining discontinuity in the density or its slope is not seen by the topological algorithms. Keeping the muffin tin radii smaller than the shortest distance from a nucleus to any critical point of the electron density is recommended. The following muffin tin sphere radii were used for the calculations: Li = 2.37 au and H =1.28 au for LiH, Na = 2.5 au and H = 1.53 au for NaH. The K-mesh values in the first Brillouin zone are 10x10x10 for all systems and $R_{mt}K_{max}$ = 5 for LiH and NaH. Na = 2.0 au, Al = 1.7 au, H = 1.2 au for $NaAlH_4$, Na = 2.0 au, Al = 1.5 au H = 0.8 au for $LiAlH_4$ and Li = 2.2 au, Al = 2.0 au, H = 1.1 au for Li_3AlH_6. The K-mesh values in the first Brillouin zone are 7x7x7 and $R_{mt}K_{max}$ = 5 for $NaAlH_4$, 7x6x4 and $R_{mt}K_{max}$ = 5 for $LiAlH_4$ and 4x4x4 and $R_{mt}K_{max}$ = 5 for Li_3AlH_6. The cut-off parameter $R_{mt}\times K_{max}$ for limiting the number of the plane waves is equal to *7*, where R_{mt} is the smallest of all atomic sphere radii and K_{max} is the largest reciprocal lattice vector used in plane wave expansion. The self-consistency was achieved when the total energy was found to be stable within 10^{-4} Ry. The topological analysis of the electron density of these solid-state systems were done using CRITIC [19], a quantum theory of atoms in molecules (AIM) [8] topological code.

3. Results and Discussion

3.1. Analysis of LiH, NaH and KH

Alkali and alkaline earth metal hydrides have good hydrogen storage capacities with LiH, and NaH desorbing 12.6, 4.2 wt % of hydrogen respectively [6]. LiH, NaH and KH both crystallize in the cubic rock salt structure (space group Fm -3 m (225)), with unit cell parameters a = b = c = 4.083 Å [20], a = b = c = 4.89 Å [21] and a = b = c = 5.70 Å [22] respectively with the hydride ions occupying all the octahedral holes in an fcc array of metal ions. The DFT-optimized structures of these metal hydrides were reproduced within 2% deviation in the unit cell parameters from the experimental values. Topological analysis of LiH, KH, and NaH will be reported with references to systems such as AlH_3, MgH_2, B_2H_6, Al_2H_6 that show similar interactions [11]. Analysis of the electron density in LiH revealed two types of interactions in the solid-state structure, which is in contrast to what is indicated in the literature. There are electrostatic interactions between the Li^+ and H^- ions, with the complete transfer of 1.0 electron from lithium to hydrogen, and a novel type of H···H contact which can only be attributed to hydride-hydride

bonding in the Li–H···H–Li moieties. This is termed a hydride-hydride interaction because the hydrogen atoms involved are negatively charged. This type of interaction appears to be relatively strong, and falls within the range of electron density (0.014-0.236 e/Å^3) proposed by Popelier for dihydrogen bonding [23]. Conversely, NaH and KH exhibit only ionic interactions between the M^+ and H^- ions, with the complete transfer of 1.0 electron from the alkali metal to hydrogen. No hydride-hydride interactions are apparent in NaH and KH, presumably because of the longer distances between the hydrogen atoms in these solid-state structures (ca 3.46 Å for NaH and 4.03 Å for KH), as presented in Table 1. In addition, the smaller size of the Li^+ cation can allow for close contact between the hydrogen atoms. The homopolar hydride-hydride, H···H interactions observed in LiH can be classified as secondary type interactions that occur at distances between 2.3-3.1 Å. This hydride-hydride interaction in LiH may help in stabilizing the solid-state structure of LiH relative to NaH and KH structures.

It is important to note that a plethora of similar types of interactions (H···H interactions) were also observed in AlH_3, MgH_2, Al_2H_6, B_2H_6 and $NaAlH_4$, with some of them forming bridges between the metal centres as seen in γ-AlH_3, MgH_2, Al_2H_6, B_2H_6. These can be identified in the $Al(\mu^2\text{-}H)_2Al$ moieties in γ-AlH_3 and $Mg(\mu^2\text{-}H)_2Mg$ moiety in MgH_2 [11]. Although these interactions are considered to be weak (because they occur at distances longer than the sum of the van der Waals radius between two hydrogen atoms, 2.4 Å), they play an important role in stabilizing the extended structures of these solid-state systems due to the multiplicity in their respective unit cells. This classification is based on the distances between the hydrogen atoms involved in bonding, although distance alone is not the only criterion for accessing such interactions. The crystal structures adopted by the solid-state systems also play a significant role. On the other hand, the weaker interactions in LiH and $NaAlH_4$ are characterized by longer distances between the interacting hydrogen atoms. These H···H contacts act as additional cross-links between the hydride moieties and their combination stabilizes the solid-state systems. Some of these H···H contacts are as strong as the M–H bonds observed in these structures.

Table 1. *Topological parameters of the electron density for LiH and NaH, as obtained from WIEN2k. [Distances in Å; electron density, ρ(BCP) in e/Å^3; Laplacian, $\nabla^2\rho$(BCP) in e/Å^5].*

System	Distance	ρ(BCP)	$\nabla^2\rho$(BCP)	Charge	ε
Li–H	2.041	0.101	1.151	Li = 0.86	0.00
H···H	2.691	0.069	0.311	H = -0.86	0.79
Na–H	2.421	0.075	0.082	Na =0.80	0.00
H···H	3.423	-	-	H = -0.80	-

The chemical significance of these counter-intuitive H···H contacts is unclear but reports have shown that they play an important role in understanding the reaction coordinate leading to the release of hydrogen from these solid-state systems. Similar long-range interactions were observed between hydrogen atoms that carry very small or neutral charges as in C−H···H−C interactions [24]. Initially, doubts were expressed over the physical significance of bond paths between the hydrogen atoms in these types of interactions, but Pendás et al [19] confirmed their existence by pointing out that bond path may also be regarded as privileged exchange channels between nuclei, which help in stabilizing their mutual interactions [11]. A deeper understanding of these ubiquitous hitherto unrecognized hydride-hydride interactions will shed more light on how to improve the design and control of many other solid-state systems for hydrogen storage. In an attempt to physically identify these types of interactions, the Laplacian plot (including bond paths) for LiH and NaH are shown in Figure 1.

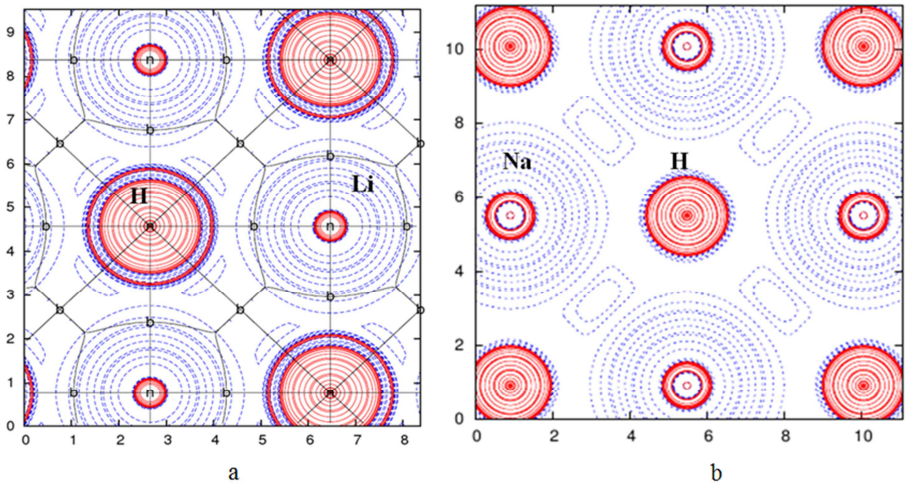

Figure 1. *Laplacian plots of the electron density in a (110) plane of LiH (a) and NaH (b). The contour intervals were set at 0.1 e/Å^3 (b = BCP).*

Figure 1 shows the Laplacian plot (including bond paths) in a (110) plane of LiH (a) and NaH (b). The electron density is concentrated on the atomic nuclei with polarizations observed on the hydrogen atoms in LiH. No such polarizations were evident in NaH. In addition a bond critical point (BCP) was identified between the hydrogen atoms in the hydride moiety in LiH. This observation confirms the previous topological results in Table 1 where H···H contacts are seen in LiH and not in NaH. For the

same reason, the size of Na^+ cation and the longer distance between the hydrogen atoms in NaH may be the determining factor preventing interaction between the hydrogen atoms. The physical existence of this type of interaction in LiH was exemplified by plotting the 3-D representing all the interactions in LiH and NaH (Figure 2). The cations are located at the corners while the anions are found at the mid-edges of the unit cell. Figure 2 shows interactions between the hydrogen atoms in the LiH, which is not evident in NaH. These are represented by the presence BCPs between the interacting hydrogen atoms (H···H contact), with no H···H interactions observed in NaH. In a similar manner, these H···H contacts were also absent in KH and this trend is expected to continue down the group. This can be attributed to the increase size of the alkali metal cations, M^+ down the group, thus leading to longer distances between the hydrogen atoms.

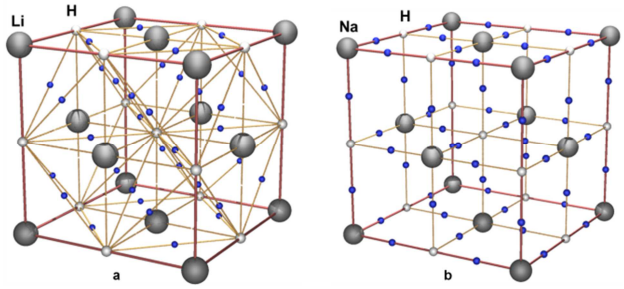

Figure 2. *3-D plots showing interactions in (a) LiH, and (b) NaH structures. There exist H···H interactions in (a), indicated by the presence of a BCP (blue), with no such interactions in (b).*

3.2. Analysis of $NaAlH_4$, $LiAlH_4$ and Li_3AlH_6

Among the complex metal hydrides, $LiAlH_4$ and $NaAlH_4$ are the most studied solid-state structures for hydrogen storage, with $LiAlH_4$ being the most promising candidate. $LiAlH_4$ releases 7.9 wt % H_2 in a two-step process, whereas $NaAlH_4$ releases 5.6 wt % H_2 in the first two steps [25]. This is due their high hydrogen storage capacity, portable power potential and low production costs.

$NaAlH_4$ crystallizes in the tetragonal body-centred space group I 41/az (88) with unit cell parameters a = b = 5.0251 Å and c = 11.3539 Å [26]. The crystal structures of $NaAlH_4$, $LiAlH_4$ and Li_3AlH_6 are shown in Figure 3. The DFT-optimized structural coordinates of $NaAlH_4$ are in excellent agreement with experimental values, with only a slight deviation (1.6% expansion) in the unit cell parameters. The structure of $NaAlH_4$ is composed of isolated $[AlH_4]^-$ tetrahedra surrounded by Na^+ cation. The Al atoms in $NaAlH_4$ are tetrahedrally coordinated to the hydrogen atoms in the $[AlH_4]^-$ tetrahedral environment, as opposed to the octahedral environment in AlH_3. The topological analysis of the electron density revealed a plethora of interactions in the solid-state structure of $NaAlH_4$ and the intermediate phase Na_3AlH_6, which contribute to the stabilization of the solid-state structure. The Al–H bonds in $NaAlH_4$ are stronger than those observed in AlH_3 as revealed by the shorter bond distance (ca. 1.63 Å) and a high value of the electron density (0.48 e/Å^3) at the BCP between aluminum and hydrogen in $NaAlH_4$. The topological parameters and the charges indicate a strong ionic bonding between aluminum and hydrogen (Al–H). The ionic character in the Al–H bonds is greater than the covalent character on account of the polarized nature of the H-atoms (Figure 4). This finding is in contrast to the general notion that Al and H are held together by covalent interactions in AlH_3 and $NaAlH_4$. The hydrogen atoms in $NaAlH_4$ are also involved in two distinct types of ionic Na–H interactions and these ionic interactions are almost as strong in strength as those observed for Na–H bonds in crystalline NaH. This can be confirmed by the values of their electron density at the BCP and/or bond distances in the Na−H bond (0.056 e/Å^3 and 2.44 Å and 0.075 e/Å^3 and 2.44 Å for $NaAlH_4$ and NaH respectively [11, 23].

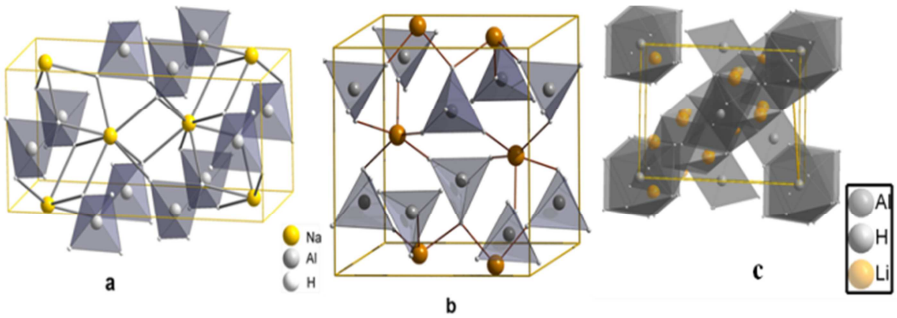

Figure 3. *Computed crystal structures of (a) $NaAlH_4$; (b) $LiAlH_4$; and (c) Li_3AlH_6.*

Furthermore, a range of unusual but significant H···H contacts (hydride-hydride interactions) were also observed in the solid-state structure of $NaAlH_4$. These H···H interactions serve as cross-links between the $[AlH_4]^-$ tetrahedra (Figure 4b). These interactions are not very strong (because of modest electron density values at the BCPs, 0.026-0.058 e/Å^3), but their combine effects (multiplicity of 40 in the unit cell) are significant. These interactions are comparable in strength ρ(BCP) to the range of dihydrogen bonds (0.014 e/Å^3-0.236 e/Å^3), [$H^{\delta+}$···$H^{\delta-}$] proposed by Popelier [23]. They exist in the range 2.735-3.086 Å, again demonstrating that distance alone is not the controlling factor that determined the existence of these interactions. The threshold for these secondary types of interactions may be set at 3.1 Å, with distances below 2.5 Å representing very strong interactions as observed in γ-AlH_3 and β-MgH_2. The unique chemical nature of the hydrogen atom with its single $1s^1$ valence electron can permit it to engage in a wide range

of unconventional bonding interactions even at distances greater than twice its van der Waals radius (2.4 Å). This is due to the large size of the hydridic hydrogen atom and its high degree of polarizability. Similar hydride-hydride interactions are also observed in the intermediate Na_3AlH_6, but here they are weaker than those observed in $NaAlH_4$. This is because the intermediate hexahydride (Na_3AlH_6) is less stable with respect to the strength of interactions and energy compared to $NaAlH_4$. The interactions are termed hydride-hydride, or homopolar, interactions because the hydrogen atoms engaged in bonding are negatively charged. Therefore, the release of hydrogen from these systems can be mediated through the strengths of the Al–H···H–Al and/or Na–H···H–Na interactions. To get a better understanding of these interactions, the Laplacian of the electron density and 3-D structural plots are shown in Figure 4 and 5. In Figure 4, the hydrogen atoms are seen to be polarized, on account of their ionic interactions with Al and Na. Figure 4b shows the cross-linking interactions between the H···H interactions and the $[AlH_4]^-$ tetrahedra. The 3-D plots (Figure 5) show the different types of H···H interactions, which are revealed by the presence of BCPs between the two interacting H atoms. These interactions are seen as cross-links between the $[AlH_4]^-$ tetrahedra, and their combined effects stabilize the extended solid-state structure of $NaAlH_4$. These range of interactions are counter-intuitive because the hydrogen atoms carry the same charge, but at the same time they are remarkably strong because of the multiplicity.

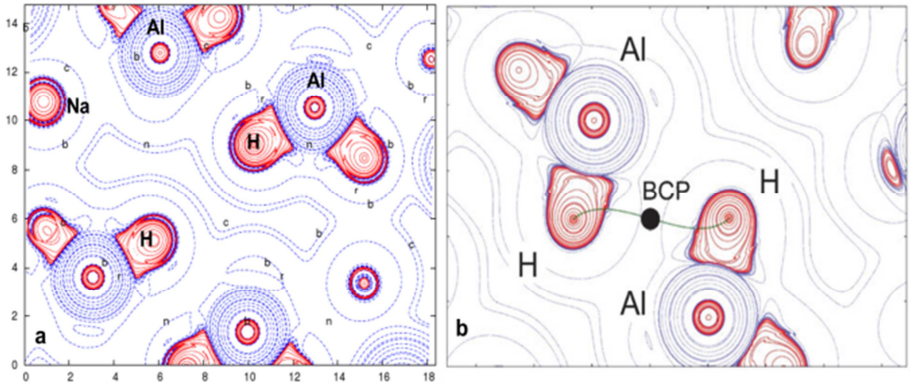

Figure 4. *Laplacian plots (a) in a plane of $NaAlH_4$ showing polarization of the H-atoms; (b) showing one of the four types of H···H interactions observed in the crystal structure of $NaAlH_4$. The contour intervals were set at 0.1 e/Å^3).*

On the other hand, $LiAlH_4$ crystallizes in the monoclinic space group P121/c (14), with unit cell parameters a = 4.825 Å, b = 7.804 Å and c = 7.897 Å [174]. The DFT-optimized structure of $LiAlH_4$ was faithfully reproduced with a deviation of less than 2% from the experimental unit cell parameters. In a similar fashion, the Al–H and Li–H interactions in $LiAlH_4$ are markedly ionic in character, with the Al–H ionic interactions being stronger than the Li–H interactions. This is seen from the electron density and positive Laplacian values in accordance with Espinosa's correlation scheme [27] (Table 2). This conclusion is confirmed by the charges on Al, Li and H, which indicate that about 80% of the valence electrons on Al and Li are transferred to H. The Al–H ionic bonds are comparable in strength to those observed in their $NaAlH_4$ counterpart, but slightly stronger than those observed for γ-AlH_3. The Li–H ionic bonds on the other hand are slightly weaker than those observed in LiH, but their overall strength is remarkable due to their multiplicity (more 40 per unit cell).

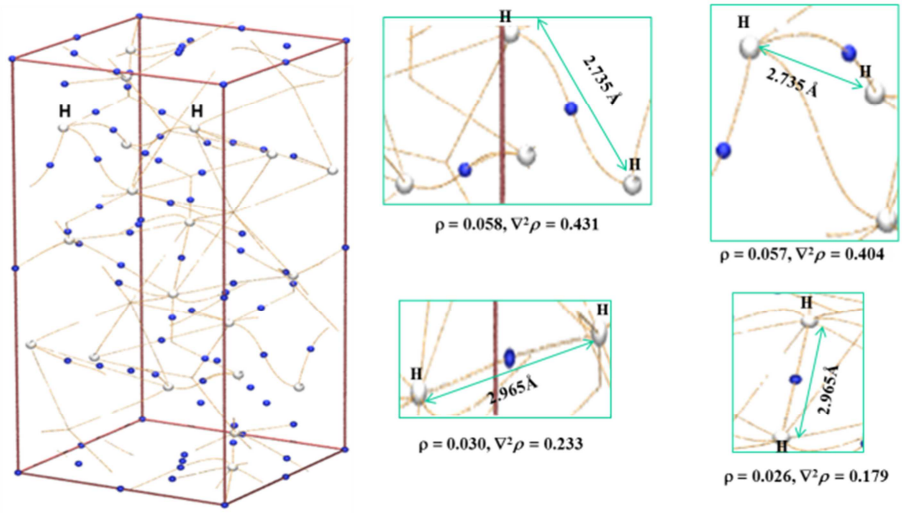

Figure 5. *3-D plot of $NaAlH_4$ showing the H···H interactions. The different types of H···H interactions are represented, including the distances. H (colourless), and BCP (blue).*

In addition to the strong ionic interactions that stabilize the $LiAlH_4$ structure, there exist a plethora of hitherto unrecognized hydride-hydride interactions in its unit cell. These interactions are remarkably stronger than those observed in their $NaAlH_4$ counterpart because of the high electron density values that exists between the two interacting H-atoms in the former (Table 2). Based on the classification of these secondary type interactions, some of these hydride-hydride interactions are very strong with bond distances well below 2.5 Å. These interactions are only similar in strength to those observed in β-MgH_2 and γ-AlH_3. In addition, their strength can also be compared to Li–H ionic bonds in LiH, Mg-H ionic bonds in MgH_2, and Al–H and Na–H ionic bonds in $NaAlH_4$. Although some of these hydride-hydride interactions are weak (bonding distance greater than 2.5 Å), their combine effect is significant. In a similar manner, the hydrogen atoms involved in bonding are all negatively charged, which implies that the release of hydrogen from this system can be mediated through the Al–H···H–Al and/or Li–H···H–Li interactions. Furthermore, the hydride-hydride interactions in $LiAlH_4$ act as cross-links between the $[AlH_4]^-$ tetrahedra. This adds to the stability of its solid-state structure. Therefore, the stability of these systems ($NaAlH_4$, Na_3AlH_6 and $LiAlH_4$) can be related to the strengths of the interactions (including hydride-hydride interactions) keeping the structures together. These interactions (ionic and hydride-hydride interactions) are stronger in $LiAlH_4$ than in $NaAlH_4$. This can be confirmed by the electron density values at the BCPs (Table 2). These results are consistent with the concept reported by Espinosa et al. [27], which states that the strength of a bond is exponentially related to the value of the electron density at the BCP and the distance between them. Figure 6 represents all the hydride-hydride interactions in $LiAlH_4$. In general, these hydride-hydride interactions may enhance or impede the release of hydrogen from these systems.

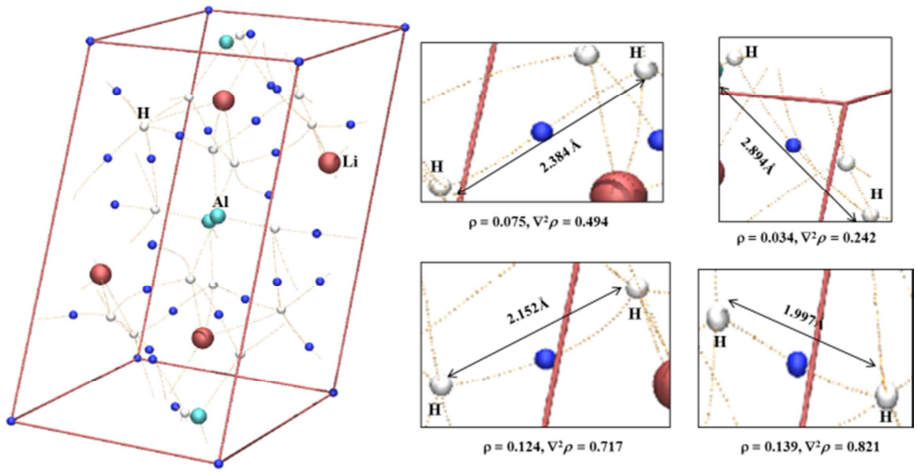

Figure 6. *3-D plot of $LiAlH_4$ showing the H···H interactions. Four different types of H···H interactions are represented including the distances. H (colourless), Al (green), Li (red-brown), and BCP (blue).*

Similar to $NaAlH_4$ and Na_3AlH_6, Li_3AlH_6, is formed as an intermediate during the hydrogenation of $LiAlH_4$ and also exhibits a number of interactions that contribute to the stabilization of its solid-state structure. Li_3AlH_6 crystallizes in the R-3H space group (148), with unit cell parameters a = b = 8.071 Å, and c = 9.513 Å [175]. The optimized unit cell coordinates of Li_3AlH_6 are in complete agreement to the experimental values with a deviation of less than 2%. Li_3AlH_6 is made up of isolated $[AlH_6]^{3-}$ octahedra surrounded by Li^+ cations. The coordination environment is similar to AlH_3 with the Al atoms coordinating octahedrally to six H atoms to form $[AlH_6]^{3-}$ octahedra. The topological analysis of Li_3AlH_6 revealed that, in addition to the normal ionic interactions that exists between Al–H and Na–H, there also exist four types of these novel H···H interactions, which contribute to the stability of the solid-state structure. The ionic bonds observed between Al–H in Li_3AlH_6 are slightly weaker than those seen in their $NaAlH_4$ and $LiAlH_4$ counterparts, but similar in strength to those in α-, β- and γ-AlH_3. This can be confirmed by the values of the electron density at the BCPs and the longer bond distances between the interacting atoms in Li_3AlH_6. (Table 2). On the other hand, the Li–H ionic bonds are similar in strength to those found in $LiAlH_4$, but weaker than the Li–H ionic bonds in LiH. Similar to the other solid-state systems, $NaAlH_4$ and $LiAlH_4$, Li_3AlH_6 revealed a range of secondary hydride-hydride interactions. These interactions are slightly weaker than those observed in $LiAlH_4$, but similar in strength to those found in $NaAlH_4$. The bond distances in these novel type interactions ranged from 2.3-2.7 Å, which means that they can be viewed as strong-to-moderate interactions. In addition, these H···H interactions also contribute to the stability of the extended structure of Li_3AlH_6. They are weaker than those observed for $LiAlH_4$ (Table 2).

The above results confirm the fact that Li_3AlH_6 exists as an intermediate (decomposing around 127 °C) during the decomposition of $LiAlH_4$. The stability of this systems leads to the release of 2.6 wt % H at a slightly higher temperature. In general, all the Al–H interactions in the alanate systems ($NaAlH_4$, $LiAlH_4$ and the intermediate Li_3AlH_6), are stronger than the Na–H interactions. This can be confirmed by looking

at the values of the electron density, the Laplacian of the electron density at the BCP and the distance between the interacting atoms (Table 2).

Table 2. *Topological parameters of the electron density for $NaAlH_4$, $LiAlH_4$ and Li_3AlH_6 as obtained from WIEN2k. [Distances in Å; electron density, ρ(BCP) in e/Å^3; Laplacian, $\nabla^2\rho$(BCP) in e/Å^5].*

System	Distance/Å	ρ(BCP) e/Å^3	$\nabla^2\rho$(BCP) e/Å^5	Charge	ε
$NaAlH_4$					
Al–H	1.634	0.479	3.656	Al = 2.12	0.03
Na–H	2.439	0.053	0.784	Na = 0.89	0.05
Na–H	2.439	0.056	0.817	H = -0.77	0.07
H–H	2.735	0.058	0.431		5.33
H–H	2.735	0.057	0.404		2.53
H–H	2.965	0.026	0.179		0.65
H–H	2.965	0.030	0.233		0.07
$LiAlH_4$					
Al–H_{av}	1.675	0.465	4.043	Al = 2.12	0.13
Li–H_{av}	2.181	0.081	1.006	Li = 0.89	3.54
H–H	1.997	0.139	0.821	H1 = -0.72	0.45
H–H	2.060	0.113	0.799	H2 = -0.83	0.30
H–H	2.152	0.124	0.717	H3 = -0.76	1.56
H–H	2.384	0.075	0.494	H4 = -0.70	0.19
H–H	2.838	0.112	0.405		12.71
H–H	2.894	0.034	0.242		0.40
H–H	2.949	0.033	0.225		0.27
Li_3AlH_6					
Al–H	1.734	0.373	3.078	Al = 2.26	0.02
Al–H	1.754	0.360	2.843	Li = 0.88	0.01
Li–H_{av}	2.000	0.096	1.484	Al2 = 2.16	0.29
H–H	2.344	0.080	0.364	H1 = -0.82	0.54
H–H	2.611	0.072	0.349	H2 = -0.83	0.57
H–H	2.654	0.069	0.366		0.55
H–H	2.674	0.069	0.356		0.40

4. Conclusion

Topological analysis of the electron density have been performed on the solid-state materials; LiH, NaH, KH, $LiAlH_4$, $NaAlH_4$ and Li_3AlH_6 in an attempt to fully analyze and interpret the different types of interactions that stabilize them. It is observed that the stability of the solid-state systems increase with the number or multiplicity of the bonding interactions in them including the unprecedented hydride-hydride interactions. LiH is seen to be more stable compared to NaH and KH. Similarly, $LiAlH_4$ is more stable than $NaAlH_4$, which in turn is more stable than Li_3AlH_6. This increase in stability is due to the multiplicity of these hydride-hydride interactions. Although the strengths of these hydride-hydride interactions are not as strong compared to the M-H counterparts, their multiplicity contributes enormously to the stability of the systems. These hydride-hydride interactions increase with the complexity of the solid-state materials. Furthermore, it is suggested that these hydride-hydride interactions play a significant role in understanding the reaction coordinates leading to the release of hydrogen in these systems for hydrogen storage applications.

Supporting Information. Details of the optimized solid state structures; Laplacian plots; 3-D plots showing the interactions can be requested from James Titah.

Author Contributions

J. T conceived, put together, and performed the DFT calculations described in this manuscript with assistance from F. C. The manuscript was written with contributions from all authors.

Funding Agencies

We are thankful to the Natural Sciences and Engineering Research Council (NSERC) of Canada and its H2CAN network for financial support.

Acknowledgements

We are indebted to Dr. Alberto Otero-de-la-Roza for his helpful suggestions and his support for using his program CRITIC.

References

[1] George, L.; Saxena, S. K. *International Journal of Hydrogen Energy*. 2010, *35*, 5454-5470.

[2] *http://www.hydrogen.energy.gov/advisory_htac.html,* HTAC Annual Report, 2010 – 2011 (accessed Nov. 10, 2011).

[3] a. Johnson, J. K., Sholl, D. S. *Annual Progress Report*, DOE Hydrogen Program, 2008, 465-470, b. Pedicini, R.; Gatto, I.; Passalaguar, E. *Solid-State Materials for Hydrogen Storage*; Nanostructured Materials for Next-Generation Energy Storage and Conversion, 2018, 443.

[4] a. Jain, I. P.; Chhagan, L.; Jain, A. *Int. Hydrogen Energy*. 2010, *35*, 5133, b. Abe, J. O.; Popoola, A. P. I.; Ajenifuja, E.; Popoola, O. M. *International Journal of hydrogen Energy*, 2019, *04*, 068.

[5] http://www1.eere.energy.gov/hydrogenandfuelcells/mypp/pdfs/storage.pdf, *Interim Update*. 2011 (accessed Nov. 11, 2011).

[6] a. Jensen, C. M.; Sun, D. L.; Srinivasan, S. S.; Kiyobayashi, T.; Kuriyama, N. *Phys. Rev. B*. 2004, *70*, 060101-1-060101-4, b. Karsten, M. *ChemBioEng Reviews*. 2019, *6, 3*, 72-80.

[7] a. Kang, X. D.; et al, *J. Alloys Compd*. 2006, *424*, 365-369, b, Mauro, F. S.; Marcello, B.; Mads, B.; Moretto, P. J. Power Sources. 2017, *342*, 853-860.

[8] Bader, R. F. W. *Atoms in Molecules- A Quantum Theory,* Clarendon Press, Oxford, 1990.

[9] Bader, R. F. W. *Chem. Eur. J*. 2006, *12*, 7769-7772.

[10] Matta, C. F.; Boyd, R. J. *An Introduction of the Quantum Theory of Atoms in Molecules*. 2007, 1-25.

[11] Peter, S.; Franklin, N. C.; James, T. T.; McGrady, G. S. *Chem. Eur. J.* 2012, *18*, 9476-9480.

[12] David, J. W.; James, T. T.; Franklin, N. C.; Traboulsee, T.; Flogeras, J.; McGrady, G. S. *J. Am. Chem. Soc.* 2011, *133*, 16598-16604.

[13] a. Popelier P. L. A, Joubert L., D. S. Kosov J. Phys. Chem. A 2001, *105*, 8254-8261, b. James, T. T.; Franklin C. N.; Peter S.; Coulibaly W. K.; Mamadou G. R. K. *International Journal of Computational and Theoretical Chemistry.* 2019*, 7*, No. 2, 115-120.

[14] Martin Pendas A. J. Chem. Phys. 2002, *117*, 965-979, b. Remi C., Christine L., Bernard S., *Applications of Topological Methods in Molecular Chemistry*, 2016, 59-63.

[15] Blaha, P.; Schwarz, K.; Madsen, G. H.; Kvasnicka, D.; Luitz, J In: Schwarz K (ed) FP-L/APW + lo programme for calculating crystal properties, Technische Universität Wien, Vienna, 2001.

[16] Perdew, J. P.; Burke, S.; Ernzerhof, M. *Phys. Rev. Lett*. 1996, *77*, 3865.

[17] Desclaux, J. P. *Comput. Phys. Commun*. *1*. 1969, 216.

[18] Koelling, D. D.; Harmon, B. N. *J. Phys. C* 1977, *10*, 3107, b. Peter S.; Franklin C.; James T.; Sean McGrady *Chem. Eur. J*. 2012, *18*, 9476-9480.

[19] Martin Pendas; Luana, V. *The critic program*, 1995-2003.

[20] Calder, R. S.; Cochran, W.; Griffithis, D.; Lowde, R. D. *J. Phys. Chem. Of Solids*. 1962, *23*, 621-632.

[21] Shull, C. G.; Wollan, E. O.; Morton, G. A.; Davidson, W. L. *Phys. Rev*. 1948, *73*, 842-847.

[22] Taber, D. F.; Nelson, C. G. *J. Org. Chem*. 2006, *71*, 8973–8974.

[23] Popelier, P. L. A. *J. Phys. Chem. A,* 1998, *102*, 1873-1878.

[24] Custelcean, R.; Jackson, J. E. *Chem. Rev.* 2001, *101*, 1963.

[25] Liu, X.; McGrady, G. S.; Langmi, H. W.; Jensen, C. M. *J. Am. Chem. Soc.* 2009, *131*, 14, 5032-5033.

[26] Fichtner, P.; Frommen, M.; Leon, C. *J. Phys. Chem. B*, 2006, *110*, 3051-3054.

[27] Espinosa, E.; Molins, E.; Lecomte, C. *Chem. Phys. Lett*. 1998, *285*, 170-173.